Journal of Chemical Health Risks

www.jchr.org

JCHR (2026) 16(2), 1217-1226 | ISSN:2251-6727

# Photocatalytic Degradation of Bg by Zr Doped $Co_3O_4$ Nanoparticles

**K. S. Ramya and B. Karthikeyan***

Department of Chemistry, Annamalai University, Annamalai nagar, Tamilnadu- 608 002, India.

***(Received: 16 January 2026 Revised: 25 February 2026 Accepted: 17 March 2026)***

**KEYWORDS**

Morphological study, Sun and UV Light

**ABSTRACT:** The synthesis of $Co_3O_4$ and Zr-$Co_3O_4$ nanoparticle using a co-precipitation method for efficient photocatalytic degradation of Brilliant green (BG) dye under UV and natural sunlight. Characterization through, Elemental mapping of FE-SEM, HR-SEM, XRD, HR-TEM, EDAX, PL and UV-DRS techniques confirmed the successful synthesis and structural integrity of the materials sheet-like structures and Chain spherical, tetragonal structures for Zr-$Co_3O_4$ and Zr-$Co_3O_4$ and while the composite maintained the crystallinity of both phases, Low intensity very high Photocatalytic activity by PL aand UV-DRS analysis demonstrated a reduction in the band gap from 3.3 eV ($Co_3O_4$) to 2.6 eV (Zr- $Co_3O_4$) enhancing photocatalytic efficiency. Photocatalytic degradation tests indicated Zr-$Co_3O_4$ achieved (98% Natural sun light) Brilliant green (BG) removal, outperforming Zr-$Co_3O_4$ (96% UV) this performance enhancement is attributed to the synergistic interaction between Zr-$Co_3O_4$ nanoparticles under solar irradiation,

**Introduction**: The current living standards, coupled with a growing population, have resulted in a notable rise in the demand for vital resources, including food, water, energy, and raw materials, across multiple industrial sectors. A significant array of strategies has been formulated to eliminate synthetic dyes from wastewater to mitigate their environmental impact. Each year, more than 70,000 tons of approximately 10,000 varieties of colors and shades are distributed globally. Approximately 20–30% of colors are wasted in mechanical effluents during the processes of material coloring and finishing through the undoped $Co_3O_4$ and doped Zr- $Co_3O_4$

**Methods**:. Synthesis of Zr-doped $Co_3O_4$nanoparticles by A straight forward co-precipitation method

**Results**: . Photocatalytic degradation tests indicated Zr-$Co_3O_4$ achieved (98% Natural sun light) Brilliant green (BG) removal, outperforming Zr-$Co_3O_4$ (96% UV) this performance enhancement is attributed to the synergistic interaction between Zr-$Co_3O_4$ nanoparticles under solar irradiation,

**Conclusions**:

Using the precipitation approach, we were then able to successfully synthesize Zr-doped $Co_3O_4$ nanomaterial. This nanomaterial was examined using an HR-SEM, which showed that the Zr-doped $Co_3O_4$. nonamaterial has a well-defined multilayer structure. An X-ray (EDX) study also verified that Zr, Co and O are present in the nanomaterial. When the generated the generated spherical-like and flower structure nanomaterial PL to $Co_3O_4$ a significant photocatalytic activity is observed. Because of its low band gap energy, the UV-Vis DRS spectrum is a good choice for photocatalysis. In the end, the photocatalytic efficiency of BG dye was found to be almost Zr-doped $Co_3O_4$ higher than photocatalytic activity that of $Co_3O_4$. After providing a workable procedure and thoroughly reviewing the created nanomaterial for industrial use, it was shown to be stable and reusable by highest catalytic ability of the Zr-doped $Co_3O_4$ nanoparticles.

## 1. Introduction

The current living standards, coupled with a growing population, have resulted in a notable rise in the demand for vital resources, including food, water, energy, and raw materials, across multiple industrial sectors. A significant array of strategies has been formulated to eliminate synthetic dyes from wastewater to mitigate

Journal of Chemical Health Risks
www.jchr.org
JCHR (2026) 16(2), 1217-1226 | ISSN:2251-6727

their environmental impact. Each year, more than 70,000 tons of approximately 10,000 varieties of colors and shades are distributed globally. Approximately 20–30% of colors are wasted in mechanical effluents during the processes of material coloring and finishing [1]. The majorities of dyestuffs, including azo colors, are toxic and must be removed before being discharged into receiving waters, as their effluents can reduce light penetration and hinder photosynthesis [**2**]. In the past ten years, photocatalytic degradation processes has been utilized extensively as methods for the deletion of whole pollutants in wastewater and effluents, particularly the degradation of dyes [**3–11**]

Spinel cobalt oxide ($Co_3O_4$), known for its high thermodynamic stability, presents promising applications across various significant technological domains. This encompasses heterogeneous catalysis for carbon monoxide oxidation and the degradation of industrial contaminants, along with anode materials in lithium-ion rechargeable, sensor advantages, pigments, batteries, and energy storage applications. Nonetheless, insufficient performance across diverse applications presents a significant challenge for scaling this material to an industrial level. Nano-structured $Co_3O_4$ has demonstrated remarkable catalytic properties, primarily due to its morphology, dimension, large surfacetovolume atomic ratio, and shapedependent characteristics, as these factors significantly affect the preferentially exposed catalytic sites [**12**].Cobalt oxide nanoparticles serve as effective semiconductor materials for photocatalytic activity. Cobalt oxide nanoparticles exhibit a suitable band gap [13-16]. The incorporation of dopants in semiconductors represents a significant method to enhance their photocatalytic performance. The removal of various dyes can be enhanced through the doping of metals like $Ni^{2+}$ and $Co^{2+}$ [**17, 18**].

This study focuses on the synthesis of nanoparticles of $Co_3O_4$ catalysts. The impact of size distribution of nanoparticles on catalysis was investigated by analyzing their catalytic performance in the degradation of BG dye.

## 2. Objectives

- To prepare modified photocatalysts*viz*. $Co_3O_4$ and Zr-doped $Co_3O_4$
- To characterize these nanomaterials using using SEM., EDX, XRD, PL and UVDR Squantifications.
- To study the activity of the prepared materials $Co_3O_4$ and Zr-doped $Co_3O_4$ by the photocatalytic decomposition of Brilliant Green (BG) dye in aqueous solution under UV and solar light irradiation.
- To study the effect of the various rate influencing factors on the photodegradation of BG
- To investigate the mechanism of the degradation
- To demonstrate the antibacterial activity of (a) $TiO_2$&Zr-doped $TiO_2$,(b) $SnO_2$&Zr-doped $SnO_2$ (c) $Co_3O_4$& Zr-doped $Co_3O_4$and (d)ZnO&Zr-doped ZnOnanocomposites against $G^{+Ve}$ and $G^{-Ve}$ bacterial strains.
- To demonstrate the photovoltaic characteristics of the modifiedphotocatlysts by Dye Sensitized Solar Cells (DSSCs).
- To test the stability and reusability of the catalysts
- To compare the photocatalysts and propose the general mechanism for the synthetic and commercial dyes

## 3. Methods

### 3.1 MATERIALS

Zirconium chloride ,Titanium (IV) isopropoxide, , Oxalic acid, Stannous chloride pentahydrate, Cobalt nitrate, Zinc nitrate, $NH_3$ solution, nitric acid ($HNO_3$-65%), Brilliant Green (BG) and ruthenium dye (535-bisTBA, N719) were utilized in their received form. Isopropyl alcohol and coumarin were sourced from Sigma Aldrich and utilized as specified. The solutions were prepared using $H_2O$.

### 3.2 Synthesis of Zr-doped $Co_3O_4$nanoparticles

A straight forward co-precipitation method combined with sonication was employed to synthesize a Zr-doped $Co_3O_4$nanocomposite material. Zirconium chloride (0.5g) at 0.1 M was dissolved in 100 mL of DI-water (Solution A), while Cobalt nitrate (2.1g) at 0.2 M was dissolved in 50 mL of DW (Solution B). With nonstop stirring, solution B was added to solution A gradually, drop by drop, before adjusting the pH to 9 by incorporating $NH_3$ solution. The resulting solution underwent agitation for duration of 3 hours. Ultrasonic

Journal of Chemical Health Risks
www.jchr.org
JCHR (2026) 16(2), 1217-1226 | ISSN:2251-6727

treatment is applied for duration of 40 minutes to facilitate the precipitate formation. The precipitate obtained was subjected to filtration and subsequently rinsed with distilled water, ethanol, and deionized water. The precipitate was subsequently gathered and subjected to drying at a temperature of 100°C in an oven for 24 hours. The powder underwent calcination in a MF at 500°C for duration of 2 hr as presented in Scheme 1

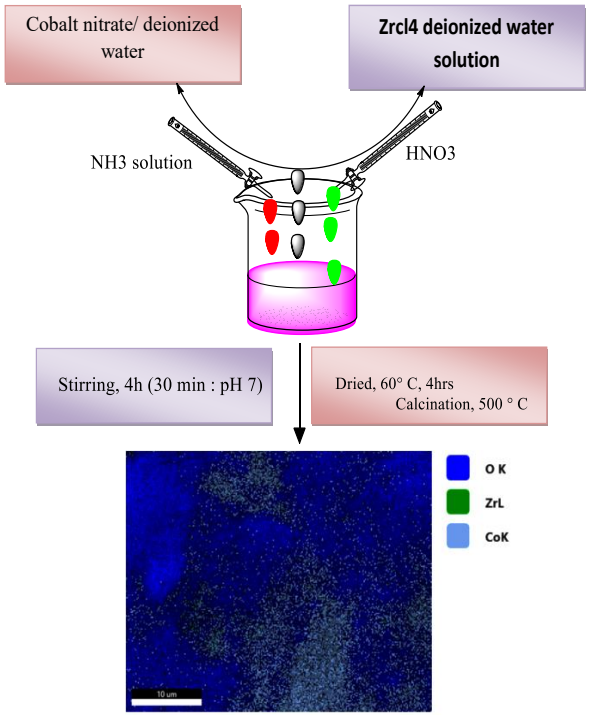


**Scheme.1.** Preparation of the Zr doped $Co_3O_4$nanoparticles

## 4. Results and Discussion

### 4.1 SEM analysis

SEM is extensively employed to examine the morphological characteristics and surface features of the catalyst surfaces.The SEM analysis of pure cobalt oxide nanoparticles prior to the photocatalytic degradation is depicted in **Figure 1**.Surface texture and porosity are evident in the SEM micrographs .Its surface micrograph also shows the microspores and mesopores with heterogeneous nature.

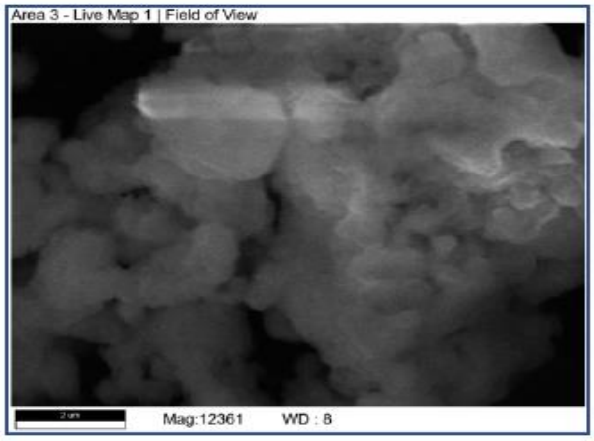


**Figure. 1** SEM image of $Co_3O_4$ nanoparticles

### 4.2 Energy-dispersive spectroscopy (EDS)

Numerous outflows are produced when an electron interacts with a test target. The distinctive X-ray emissions are analyzed using energy dispersive spectroscopy (EDS). EDS can provide material composition across a point down to a few microns. Together, these capabilities supply critical compositional data for a large assortment of materials. The analysis shows that pure and doped cobalt oxide nanoparticles have the exact natural composition of certain elements in pure cobalt oxide Co and O, as shown in**Figure.**

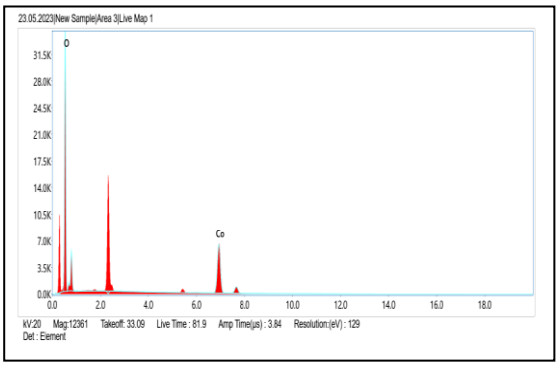


**Figure.2.**EDX analysis of $Co_3O_4$ nanoparticles

### 4.3 Elemental mapping

Elemental mapping of FE-SEM is performed to verify the composition of Co and O on the nanoparticle surface. While the FE-SEM image of $Co_3O_4$ is shown in **Figure 3a-c**,elemental mappings are displayed in **Figure 3 b and c** for Co (Block) and O (Red). As shown in

Journal of Chemical Health Risks
www.jchr.org
JCHR (2026) 16(2), 1217-1226 | ISSN:2251-6727

**Figure3a**, the densities of Co and O are uniformly distributed in the catalyst. Elemental

mapping demonstrates the catalyst consists of Co and O and its purity .

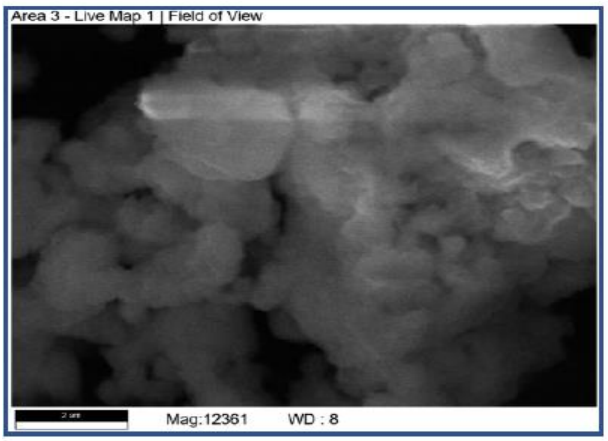


**Figure 3**. SEM image of $Co_3O_4$

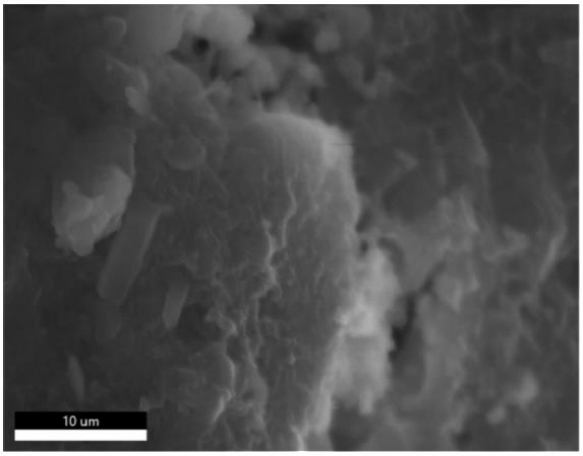


**Figure.4** SEM image of Zr-$Co_3O_4$nanomaterial

## 4.4 SEM analysis

Scanning electron microscopy is extensively employed to examine the morphological characteristics and surface features of the catalyst surfaces.The SEM analysis of Zrdoped cobalt oxide nanoparticles occurs prior to the photocatalytic degradation of GB dye, is depicted in **Figure 4**.Surface texture and porosity are evident in the SEM micrographs of both pure and doped cobalt oxide nanoparticles

### 4.5 EDS analysis

EDS is used to analyze the characteristic X-ray emissions sections into a vast range. It can provide component composition maps across a considerably larger raster zone. Together the analysis shows that Zrdoped cobalt oxide nanoparticles have the exact composition as expected Zr, Co and O as shown in **Figure 5**

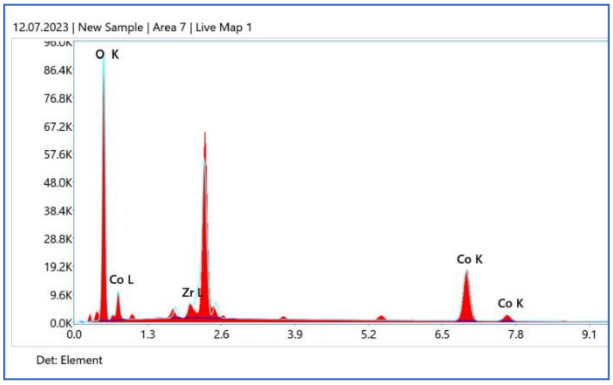


**Figure. 5** EDX spectrum of Zr- $Co_3O_4$nanomaterial

### 4.6 Elemental mapping

FE-SEM image of Zr-$Co_3O_4$ is shown in **Figure** 6 **a-d**, elemental mappings are displayed for Zr (Green), Co (Block) and O (Blue). As shown in **Figure 6a**, the densities of Zr, Co and O are uniformly distributed in the catalyst. Therefore, elemental mapping demonstrates that the catalyst consists of Zr, Co and O. It also demonstrates how pure the catalyst Zr-$Co_3O_4$

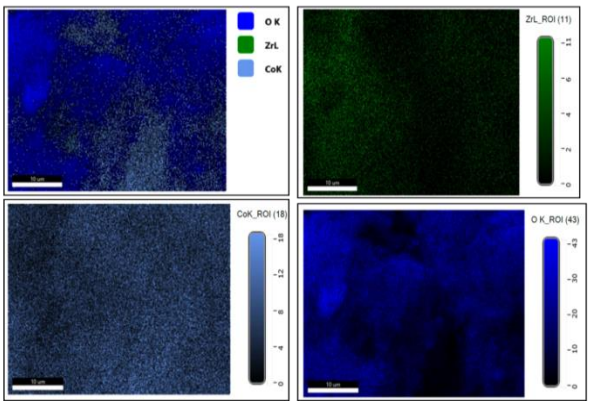


**Figure .6 ( a-d)** Elemental mapping of Zr-$Co_3O_4$.

### 4.7. HR-TEM analysis

HR-TEM images of Zr-$Co_3O_4$ nanoparticles at magnification demonstrate that the Zr-$Co_3O_4$ particles

Journal of Chemical Health Risks
www.jchr.org
JCHR (2026) 16(2), 1217-1226 | ISSN:2251-6727

have a distinctly spherical morphology with significant aggregation. Additionally, the presence of Zr is indicated as dark spots on the $Co_3O_4$ nanoparticles, as illustrated in Figure 5.7 Zr-$Co_3O_4$ at aexaggeration of 200 nm clearly exhibit lattice structures, indicating that the particles are well crystalline. Figures 7 b and c illustrate the plot profile and image profile, whereas Figure 7 d indicates an average particle size of 120 nm, with the selected particle length depicted in Figure 7 a.The previously obtained TEM designs exhibited crystallite sizes comparable to those calculated using Scherer's equation, so confirming that the synthesized Zr-$Co_3O_4$ possesses a robust crystalline structure.

### 3.8 X-ray diffraction analysis

The phase and crystalline structure of $Co_3O_4$ and Zr-$Co_3O_4$ nanoparticles are examined via X-ray powder diffraction, as illustrated in Figure 8 a and b. The diffraction peaks at 2θ values of 19.18°, 31.90°, 36.35°, 38.25° &56.13° correspond to the (111), (220), (311), (222), &(422) planes of $Co_3O_4$ (JCPDS card no. 76-1802), respectively [**19**].The diffraction peaks at 2θ values of 35.10°, 51.15°& 58.97° correspond to the (200), (220), and (311) planes of Zr (JCPDS card no. 50-1089), accordingly towards smaller angles indicates the successful Zr-doping in the $Co_3O_4$ structure. Average crystallite size of $Co_3O_4$ and Zr-$Co_3O_4$is estimated from the Scherrer's equation as about 44 and 19 nm for bare and doped catalyst. The small crystalline particle size helps for higher photocatalytic activity.

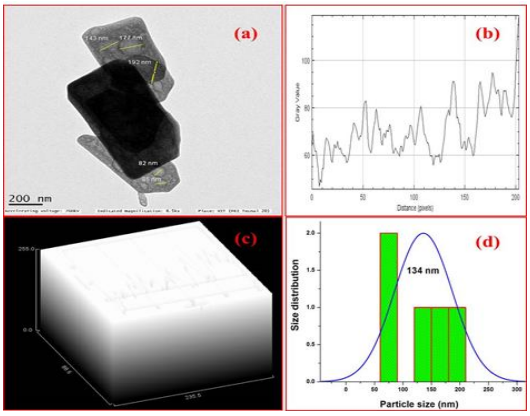


**Figure.7**TEM study of (a) Image (b) Plot profile, (c) Surface plot and (d) Particle size of Zr-$Co_3O_4$Nanoparticle

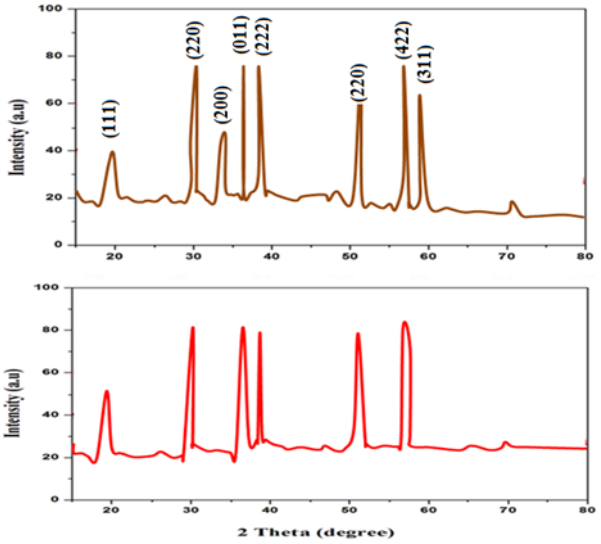


**Figure.8** XRD analysis of (a) $Co_3O_4$and (b) Zr-$Co_3O_4$nanoparticles

### 4.9 Photoluminescence analysis

Semiconductors PL spectra can show recombination, migration, and transfer of photo generated electron-hole pairs. **Figure 9a and b**shows the PL spectra of bare$Co_3O_4$ and Zr doped $Co_3O_4$. Three distinct peaks are visible at 425, 490 & 540 nm, respectively.The intensity of bare$Co_3O_4$is greater than that of Zr-doped cobalt oxide, indicating a higher rate of e- and h+ recombination. The lower intensity of Zr-$Co_3O_4$implies that Zrdoping helps successful preventing of unwanted e-/h+ pair recombination. Increasing charge carrier separation allowing more free charge carriers to participate and boosting the photocatalytic activity.

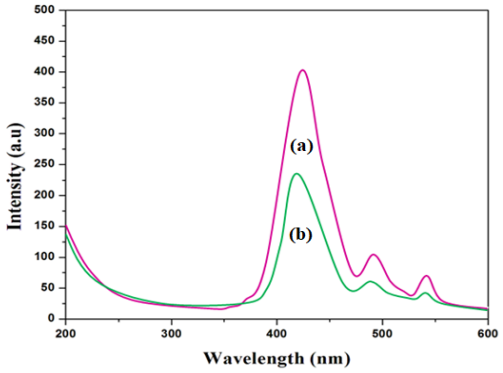


**Figure.9** PL analysis of (a) $Co_3O_4$and (b) Zr-$Co_3O_4$ nanoparticles

Journal of Chemical Health Risks
www.jchr.org
JCHR (2026) 16(2), 1217-1226 | ISSN:2251-6727

### 4.10 UV-Vis-DRS analysis

The UV-Vis-DRS for both $Co_3O_4$& the doped semiconductor oxide Zr-$Co_3O_4$ is presented in **Figure 10 a and b**. The Zr-$Co_3O_4$ exhibits enhanced absorption in both the UV & visible regions compared to $Co_3O_4$. This indicates that Zr-$Co_3O_4$ can serve as an effective semiconductor photocatalytic nanomaterial active under UV and visible light. The result $Co_3O_4$ and doped Zr-$Co_3O_4$ have been determined to be 2.7 eV and 2.25 eV, respectively.

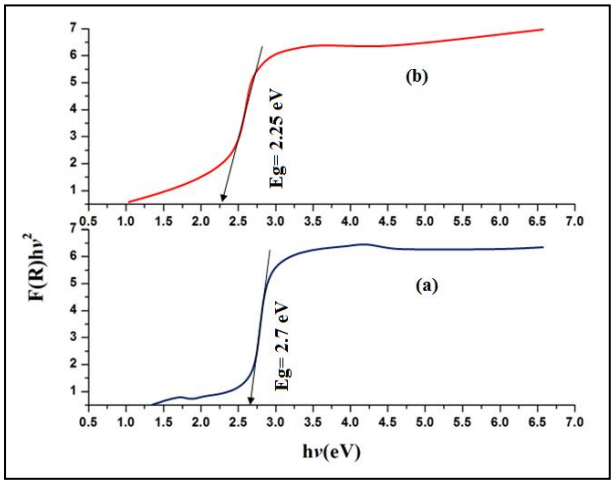


**Figure 10.**Direct band gap of (a) $Co_3O_4$and (b) Zr-$Co_3O_4$nanoparticles

## 4.11.PHOTOCATALYTIC DEGRADATION OF BG UNDER SOLARLIGHT

### 4.11.1. Preliminary analysis

The degradation of BG through photocataysis using the synthesized $Co_3O_4$ and Zr-$Co_3O_4$ catalysts is illustrated in **Figure 11**. (without nanoparticles5%). In the equal experiment, when conducted in the absence of solar light with Zr-$Co_3O_4$, there was a decrease of 10% in the dye concentration. The dye experiences a degradation rate of 96.0% when exposed to Zr-$Co_3O_4$ under solar light for duration of 60 minutes. Under identical conditions, the use of prepared $SnO_2$ resulted in only 40% of the expected degradations. This indicates that Zr-$Co_3O_4$ exhibits greater efficiency in the degradation of BG compared to $Co_3O_4$.

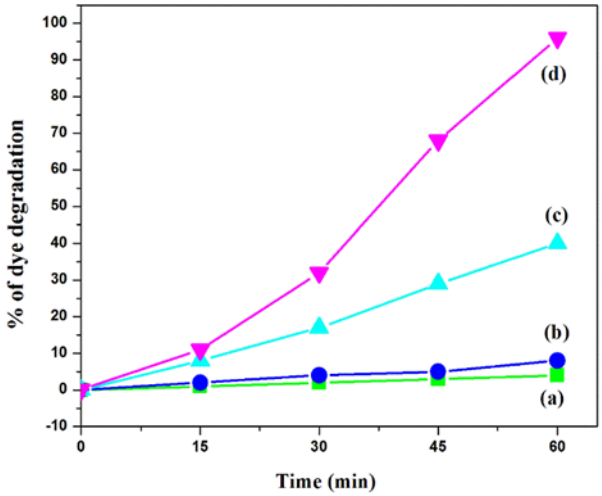


**Figure 11.** Degadation of BG dye under solar irradiation: (a) dark, (b) without catalyst, (c) $Co_3O_4$, and (d) Zr-$Co_3O_4$ catalyst.

### 4.11.2 **Influence of catalyst loading**

**Figure 12 & b** illustrates the effect of photocatalyst dosage on the degradation of BG using varying concentrations of $Co_3O_4$ and Zr-$Co_3O_4$. The degradation rises as the catalyst dosage increases. However, an excessive dosage leads to a reduction in light penetration due to the heightened light scattering effect caused by catalyst particles. The optimum result of BG dye is determined to be 0.6g, consistent with previous findings

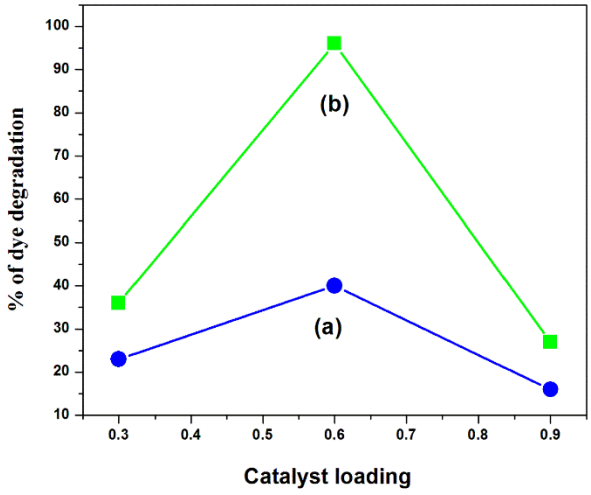


**Figure 12.** The impact of (a) $Co_3O_4$ and (b) Zr-$Co_3O_4$ catalyst

Journal of Chemical Health Risks
www.jchr.org
JCHR (2026) 16(2), 1217-1226 | ISSN:2251-6727

4.11.3 **Impact of initial dye concentration and pH influence**

**Figures 13a-d and 14a and b** illustrate the consistent trend observed under the same conditions applied in the study. As the concentration of dye rises, the quantity of dye that adheres to the catalytic surface also increases, subsequently influencing the catalytic activity of the nanocatalyst.

The influence of starting pH on BG dye is examined within the pH range of 3-11. The degradation of the dye solution shows an increase as the pH transitions from 3 to 7, followed by a subsequent decline. The result intricate for Zr-$Co_3O_4$pH 7 exhibits superior photocatalytic activity.

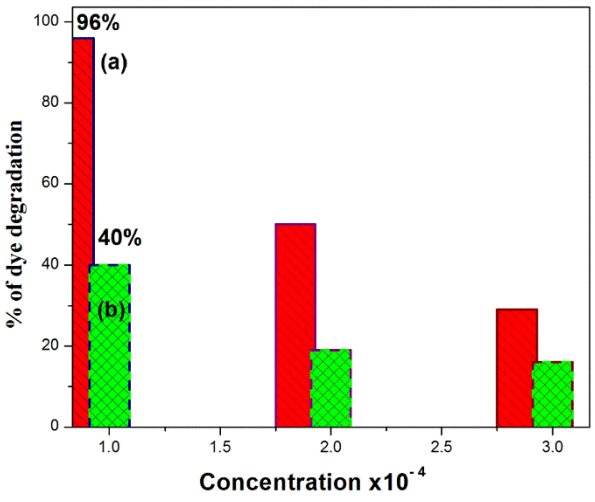


**Figure 13**(a) Zr-$Co_3O_4$and (b) $Co_3O_4$catalyst

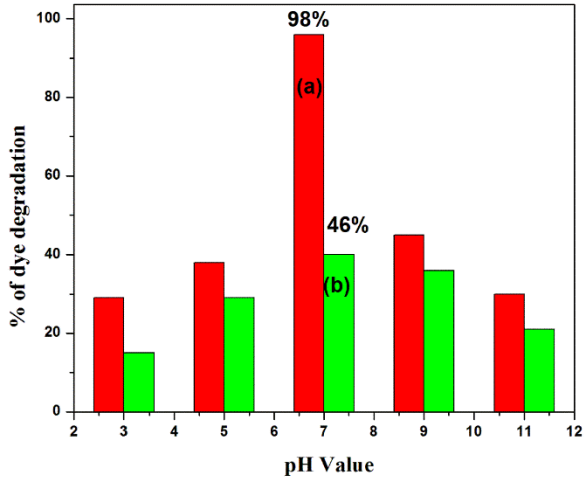


**Figure 14** (a) Zr-$Co_3O_4$and (b) $Co_3O_4$catalyst

4.11.4 **Reusability of photocatalytic activity**

As shown in the **Figure 15 a and b.**The complete degradation for 0-60 minute indicates the percentage of degradation of the $Co_3O_4$and Zr-$Co_3O_4$on BG dye as follows100, 90, 84, 81 & 81and 100, 95, 93, 90 & 90%. The outcome indicates that the doped catalyst exhibits stability and reusability, unlike the bare nanoparticles

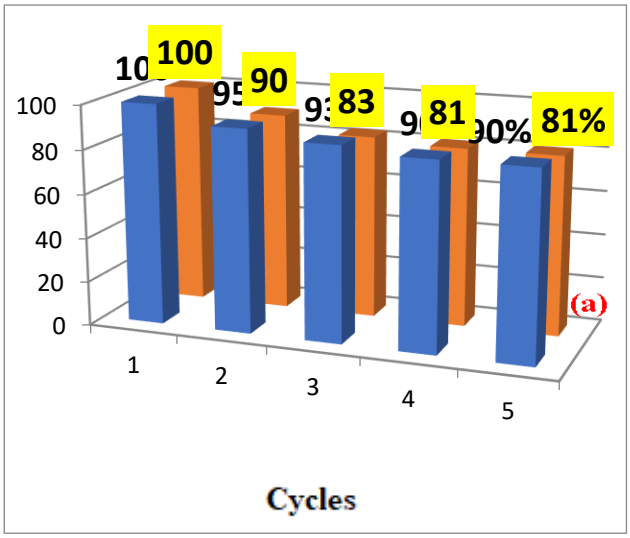


**Figure 15** Stability and reusability (a) $Co_3O_4$ and (b) Zr-$Co_3O_4$ catalyst

**4.11.5 PHOTOCATALYTIC DEGRADATION OF BG UNDER UV LIGHT**

**Preliminary analysis**

The photocatalytic degradation of BG using the synthesized $Co_3O_4$ and Zr-$Co_3O_4$ catalysts is illustrated in Figure 16. When the dye is on irradiation in the absence of a catalyst, degradation is low (0.5%). Conversely, in the same experiment conducted without UV light and with Zr-$Co_3O_4$, there is a 5% reduction in dye concentration. The dye experiences 90% degradation when exposed to Zr-$Co_3O_4$ and UV light for 60 minutes. When produced $Co_3O_4$ (Merck) was utilized under same conditions, only 35% deterioration was observed. This indicates that Zr-$Co_3O_4$ has superior efficiency in GB degradation compared to prepared $Co_3O_4$ (Merck) under UV light

Journal of Chemical Health Risks
www.jchr.org
JCHR (2026) 16(2), 1217-1226 | ISSN:2251-6727

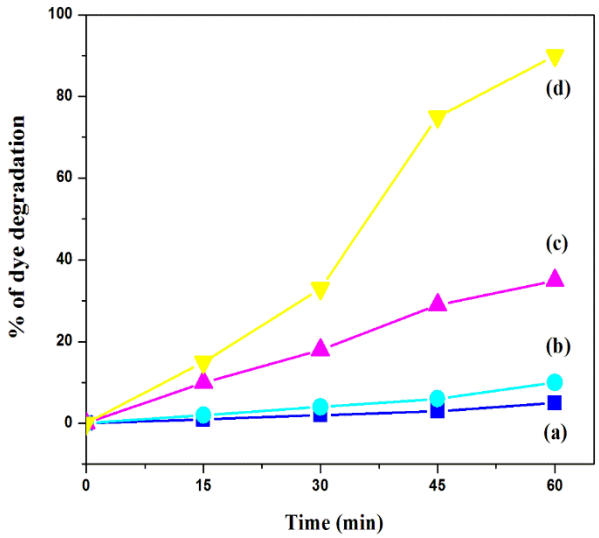


**Figure 16 D**egradation study of BG dye under UV irradiation: (a) in dark, (b) without catalyst, (c) with $Co_3O_4$, and (d) with Zr-$Co_3O_4$ catalyst.

### 3.11.6 Analysis of chemical oxygen demand (COD)

To COD measurements are conducted for the degradation of BG dye using $Co_3O_4$ and Zr-$Co_3O_4$ nanoparticles, with a loading amount of 0.6 g in a suspension of initial ion ($1\times10^{\wedge-4}$) in 40 mL of neutral pH solution, while subjected to air flow under UV and solar light irradiation. The percentage of Chemical Oxygen Demand (COD) decrease achieved by $Co_3O_4$ over 60 minutes is 35%, whereas Zr-$Co_3O_4$ demonstrates a reduction of 90% in the same timeframe. Additionally, $Co_3O_4$ shows a 41% reduction, while Zr-$Co_3O_4$ achieves a 97% reduction over 60 minutes.

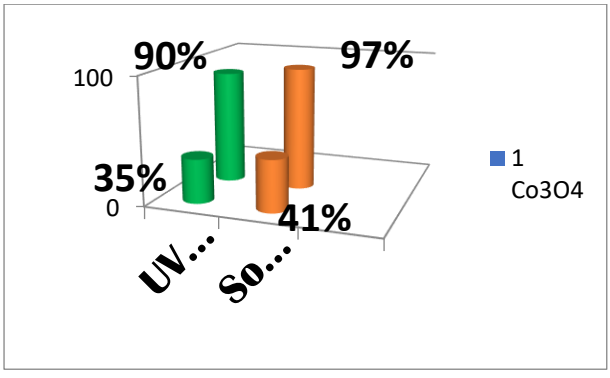


**Figure 17** COD analysis under UV and Solar Light Irradiation

### 4.11.7 Analysis of Hydroxyl Radicals

**Figures 18 a and b** demonstrate that Zr-$Co_3O_4$ has significant photocatalytic activity as evidenced by the increased fluorescence intensity, while the •OH analysis confirms that the reaction mechanism involves •OH generated from water splitting by the semiconductor metal oxides. The photocatalytic activity mechanism of Zr-$Co_3O_4$ nanoparticles is directly linked to the rate of hydroxyl radical (•OH) formation.

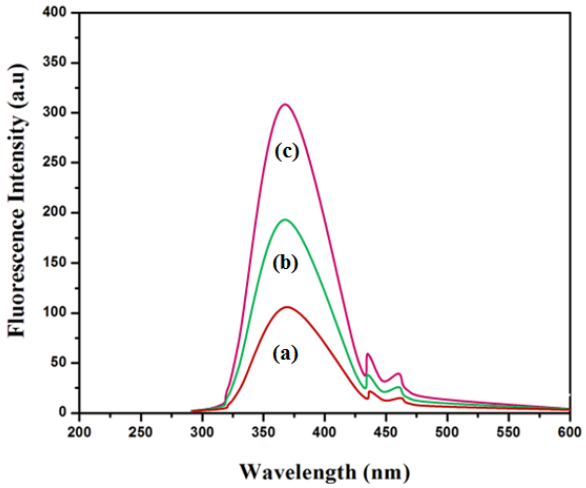


**Figure 18.** Fluorescence spectra recorded at $\lambda_{max}$ = 310 nm for Zr-doped $Co_3O_4$: (a) 0, (b) 30 & (c) 60 minutes.

### 4.12 ANTIMICROBIAL EFFICACY

$Co_3O_4$ and Zr-doped $Co_3O_4$ nanoparticles exhibit significant antibacterial action against G $^{+Ve}$& G $^{-Ve}$*S. aureus*&*E. coli*as demonstrated in Table 5.1 and Figure 19.The table illustrates the enhanced antibacterial activity of the Zr-doped $Co_3O_4$nanocomposite material

**Table 1**.Antibacterial efficacy against Gram-positive and Gram-negative microorganisms with the disc diffusion method

| S. No. | Bacteria- G $^{+Ve}$& G $^{-Ve}$ | Standard disk | (mm) | | |
|---|---|---|---|---|---|
| | | | 1 [$Co_3O_4$] | 2 [Zr-doped $Co_3O_4$] | Control (DMSO) |
| 1 | *Staphylococcus* | 25 | 11 | 20 | 20 |

Journal of Chemical Health Risks
www.jchr.org
JCHR (2026) 16(2), 1217-1226 | ISSN:2251-6727

| | | | | | |
|---|---|---|---|---|---|
| | *aureus*(Positive) | | | | |
| 2 | *Escherichia coli*(Negative) | 25 | 13 | 18 | 18 |

***Ciprofloxacin**

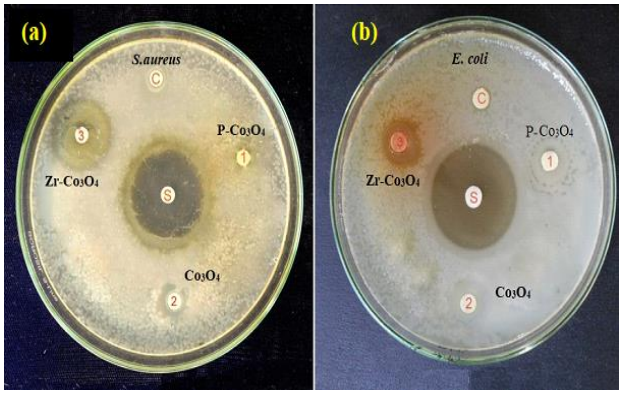


**Figure 19** Antibacterial activityof (a) $Co_3O_4$ and (b) Zr-$Co_3O_4$ nanoparticles by disc diffusion method against (a)*S.aureus*and(b) *E.coli*

### 4.13 DYE SENSITIZED SOLAR CELLS (DSSCS)

The Zr-doped $Co_3O_4$ utilized in the fabrication of a typical solar cell employing Ruthenium dye exhibits superior electro-efficiency in terms of short-circuit current density compared to $Co_3O_4$.The Zr-doped $Co_3O_4$ exhibits a Jsc value of (4.5 mA/cm²), whereas the $Co_3O_4$ displays a Jsc value of (4.0 mA/cm² [**20,21**].

**Acknowledgements Nil.**

**Funding** The authors declare that no funds, grants, or other support were received during the preparation of this manuscript.

**Declarations**

**Conflict of interest** The authors have no relevant financial or non-financial interests to disclose.

**Compliance with Ethical Standards**

The authors declare that they have no conflict of interest. This research and the manuscript are original and unpublished. All authors have read and approved the final version of the article

**Author contributions**

Corresponding Author: **B. Karthikeyan,** Annamalai University Department of Chemistry

**Refrences**

1. R. Patil, Manohar V.S. Shrivastava, Der Chem Sin, 2014, **5**, 8–17
2. H. Guo, Y. Ke, D. Wang, K. Lin, R. Shen, J. Chen, W. Weng, J Nanopart Res **15**, 1475 (2013)
3. C. Van Nguyen, Nanosci Nanotechnol, 2014, **5**, 035014-19
4. K. Vinodgopal, Environ Sci Technol, 1995, **29**, 841–845
5. S.A. Abo-Farha, Researcher, 2010, **2**(7), 1–20
6. T. Soltani, M.H. Entezari, Ultrason Sonochem, 2013, **20**, 1245–1253
7. W.P. Wang, S.P. Kalck, I.L. Faria, J Mol Catal A, 2005, **235**, 194-199
8. R. Marandi, K. Mahanpoor, A.A.M. Sharif, A.E. Olya, R. Moradi, J Basic Appl Sci Res, 2013, **3**, 347–357
9. K.M. Joshi, B.N. Patil, D.S. Shirsath, V.S. Shrivastava, Adv Appl Sci Res, 2011, **2**, 445–454
10. M. Kulkarni, P. Thakur, Int J Eng Res Gen Sci, 2014, **2**, 245–254
11. P.P. Hankare, A.V. Jadhav, R.P. Patil, K.M. Garadkar, I.S. Mulla, R. Sasikala, Arch Phys Res, 2012, **3**(4), 269–276
12. T. Warang, N. Patel, R. Fernandes, N. Bazzanella, A. Miotello, Appl. Catal. B: Environ. 2013, 132, 204–211
13. F. Azhdari, M.M. Ghaz, Adv Environ Technol, 2016, **2**, 77–84
14. Z.M. El-Bahy, M.M. Mohamed, F.I. Zidan, M.S. Thabet, J Hazard Mater. 2008, **153**, 364–371
15. S.B. Narde, R.B. Lanjewar, S.M. Gadegone, M.R. Lanjewar, Der Pharma Chem, 2017, **9**, 115–120
16. O. Sharma, M.K. Sharma, Int J ChemTech Res, 2013, **5**, 1615–1622
17. M. Mukhtar, L. Munisa, R. Saleh, Mater Sci Appl, 2012, **3**, 543–551

Journal of Chemical Health Risks

www.jchr.org

JCHR (2026) 16(2), 1217-1226 | ISSN:2251-6727

18. K. Esquivel, M.G. Garc, F.J. Rodr, L.A. Ortiz-Frade, L.A. Godinez, J Appl Electrochem, 2013, **43**, 433–440
19. Y. Wang, L. Zhou, X. Duan, H. Sun, E.L. Tin, W. Jin, S. Wang, P Catal. Today 2015,258, 576-584
20. J. Kamalakkannan, V.L. Chandraboss, S. Prabha, B. Karthikeyan and S. Senthilvelan, *J. Mater. Sci. Mater. Electron.*, **015**, 4050 (2015);
21. Y. Zhang, L. Wang, B. Liu, J. Zhai, H. Fan, D. Wang, Y. Lin and T. Xie,*Electrochim. Acta*, **56**, 6517 (2011);

.